Journal of Nuclear Materials 386–388 (2009) 319–322

Contents lists available at ScienceDirect

Journal of Nuclear Materials

journal homepage: www.elsevier.com/locate/jnucmat

Numerical investigation by finite element simulations of the ball punch test: Application to tempered martensitic steels

E.N. Campitelli [a], P. Spätig [b,*], J. Bertsch [c]

[a] Institut de Physique de la Matière Complexe, Groupe de Spectroscopie Mécanique, EPFL, CH – 1015 Lausanne, Switzerland
[b] Fusion Technology Materials CRPP–EPFL, Association EURATOM-Confédération Suisse, 5232 Villigen PSI, Switzerland
[c] Laboratory for Materials Behavior, Nuclear Energy and Safety Research Department, Paul Scherrer Institute, 5232 Villigen PSI, Switzerland

A B S T R A C T

The effects of the post-yield behaviour on the shape of small ball punch test (SBPT) curves were investigated with finite element simulations from which the load–deflection curves were extracted. We have shown the general yield load defined on the ball punch curves depends on the post-yield behaviour and that the usual linear calibration between the yield load and the yield stress may lead to erroneous estimations of the irradiation hardening. A new calibration procedure has been proposed to determine the yield stress from a ball punch curve that makes use of empirical parameters that minimizes the effects of the post-yield behaviour which influence the overall shape of the ball punch test from the very beginning of the tests.

© 2009 Elsevier B.V. All rights reserved.

1. Introduction

The tempered martensitic steels are among the most promising candidate materials for structural applications in a fusion reactor [1–4]. As the other body-centered cubic metals and alloys, they undergo a ductile to brittle transition in their fracture mode with decreasing temperature. The small ball punch test technique is a technique developed with the purpose to study the flow properties of the alloys in the unirradiated and irradiated condition [5–7] and to determine the ductile to brittle transition temperature [8]. The main motivation for using this technique is to minimize the specimen size due to the space limitations of the current irradiation facilities and of the anticipated high-energy neutron source for fusion materials IFMIF [7].

In this paper we present numerical results obtained with finite element simulations of ball punch tests and address the effects of post-yield behaviour on the calibration between the yield load, measured by ball punch tests, and the yield stress.

2. Finite element simulations

An axisymmetric model for the small ball punch test was developed using ABAQUS 6.4-1 standard code. ABAQUS models the effect of the multi-axial stress state using the von Mises stress potential and associated J_2 flow law. The details of the model can be found in [5]. It includes the ball, the upper die, the lower die and the sample disk. The ball and dies were implemented as rigid bodies. The disk was modelled with 2000 axisymmetric linear reduced integrations. A force was applied between the upper and the lower dies during the deformation; this prevents the specimen to slip. Friction between these dies and the disk constrains the latter in the same way as in the actual experimental device. The calculations were run by imposing the vertical displacement of the ball. Calculations with a friction coefficient equal to 0.05 between the ball and the disk were considered.

3. Effect of the post-yield behaviour on the yield stress determination by punch test

Mao and Takahashi performed a series of ball punch tests on various unirradiated alloys that include tempered martensitic, reactor pressure vessel and austenitic steels [9]. They defined a yield load, P_y, on the ball punch load–deflection curve as the intersection of the two slopes of the load–deflection curve drawn on both sides of the general yielding zone. They proposed the following calibration between the yield stress $\sigma_{0.2}$, sample disk thickness t and P_y for different materials as

$$\sigma_{0.2}\ (\mathrm{MPa}) = 360\frac{P_y}{t^2}\ (\mathrm{kN/mm^2}). \quad (1)$$

However, a systematic study of the effect of the post-yield behaviour (<10% strain) on the yielding load P_y or P_y/t^2 was lacking. A priori some effects of the initial shape of the $\sigma_{pl}(\varepsilon_{pl})$ curve could be expected on P_y, since plastic deformation in the disk is introduced in the disk from the very beginning of the punch test. These effects must be quantified to be properly accounted for. This point is of primary importance because it is well known that the irradiation

* Corresponding author. Tel.: +41 56 310 29 34; fax: +41 56 310 45 29.
E-mail address: philippe.spatig@psi.ch (P. Spätig).

0022-3115/$ - see front matter © 2009 Elsevier B.V. All rights reserved.
doi:10.1016/j.jnucmat.2008.12.120

affects the overall shape of the tensile curve. In particular, the transition between the elastic to plastic regime can be more pronounced than the usual smooth transition observed in unirradiated metals, like in the tempered martensitic steels [10]. The plastic regime can also, apparently, be initiated with some strain softening, which occurs in certain metals depending on the irradiation conditions [11,12]. Therefore, we may have to deal with significant changes in the constitutive behaviour following irradiation with respect to the unirradiated condition. A well-established calibration between P_y/t^2 and $\sigma_{0.2}$ for a given material in the unirradiated condition is not necessary valid for the same material in the irradiated condition. To tackle this problem, we have undertaken a numerical study to investigate the effect of the constitutive behaviour in a systematic manner. In this way four post-yield behaviours following three different yield stresses were considered. They are representative for realistic irradiation hardening of tempered martensitic steel. Thus, 12 different constitutive behaviours were used for these simulations.

The constitutive behaviours were constructed as follows: We started with the experimental constitutive behaviours of the F82H-mod steel at room temperature represented by the black curve in Fig. 1. At this temperature the yield stress is 532 MPa. The black curve is taken as the reference curve since it corresponds to the experimental data up to $\varepsilon_{pl} = 0.06$ that are linearly extrapolated at larger strains. In this Figure, we show how the other post-yield behaviours are actually constructed. Three post-yield behaviours are generated by using exactly the same strain hardening law as that of the experimental curve; in order to vary the shape of the initial plastic regime, three points have been selected along the reference curve at plastic strains of about 0.01, 0.02 and 0.05. Then the $\sigma_{pl}(\varepsilon_{pl})$ curves were generated by considering the segments of the reference curve at the right hand side of the three points

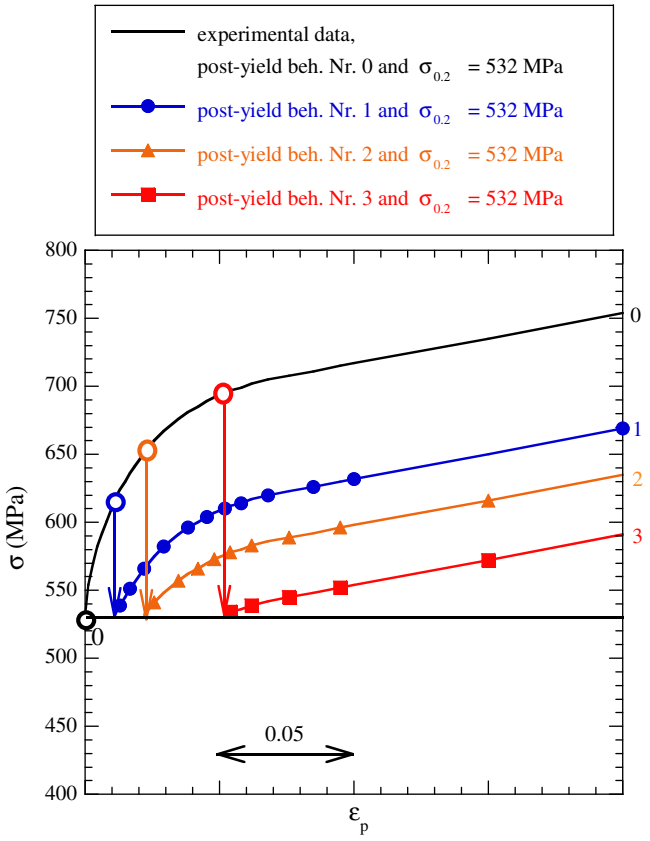

Fig. 1. Four constitutive behaviours, Nr. 0–3, used to investigate the effect of the post-yield behaviour on the determination of the yield stress by ball punch test.

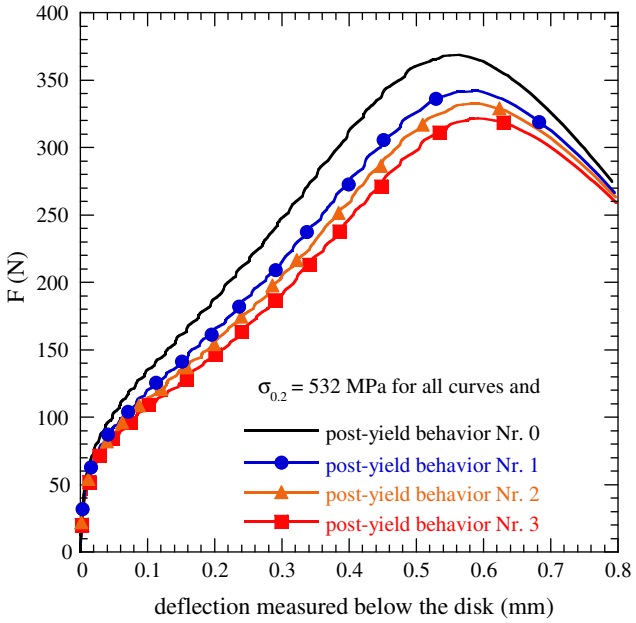

Fig. 2. SBPT curves obtained with the constitutive relationship presented in Fig. 1.

and by finally shifting these segments to the original point ($0.0\varepsilon_p$ – 532 MPa). Ultimately, ball punch test simulations were run, employing the previous $\sigma_{pl}(\varepsilon_{pl})$ curves starting at a yield stress of 532 MPa, as shown in Fig. 2, and also with the yield stresses at 632 and 732 MPa (in these cases, the curves are simply shifted in stress by 100 and 200 MPa). Therefore, in total twelve-ball punch tests calculations were carried out.

In Fig. 2, the simulated ball punch test curves obtained with the constitutive behaviours shown in Fig. 1 are plotted. It can be seen that P_y is certainly not independent of the post-yield behaviour. This point becomes even clearer in Fig. 3, where the yield stress

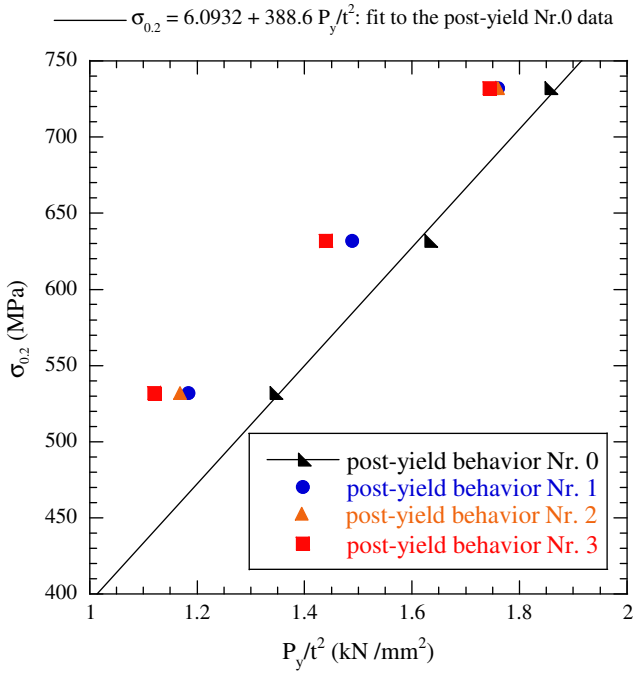

Fig. 3. $\sigma_{0.2}$ versus P_y/t^2 ($t = 0.250$ mm). Note the scatter in P_y/t^2 owing to the post-yield behaviour.

is plotted against P_y/t^2 for the 12 simulations ($t = 0.25$ mm), and where a large scatter in P_y/t^2 is found at a given yield stress. This observation indicates that P_y actually reflects a certain average flow stress level at the beginning of $\sigma_{pl}(\varepsilon_{pl})$ curve rather than only $\sigma_{0.2}$. The Fig. 3 also represents the 'resolution' we can expect on the determination of the yield stress if a calibration obtained with unirradiated materials is used. The linear fit drawn in the Fig. 3 goes through the P_y/t^2 points obtained with the post-yield behaviour Nr. 0. This fit can be regarded, in a first approximation, as the fit that would be found for a variety of unirradiated materials, which usually have a parabolic type of strain hardening with a rather smooth transition from the elastic to plastic regime. The fit in Fig. 3 considered as that of the unirradiated material is found well consistent with the calibration of Mao and Takahashi; the slope we determined is 388 against 360 (MPa/kN/mm^2) for Mao and Takahashi.

A careful analysis of Fig. 3 is instructive. First of all, it must be strongly emphasized that using the calibration done on unirradiated material to assess the irradiation hardening may lead to significant errors. We recall that the irradiation hardening is defined as the difference in the yield stress between the irradiated and unirradiated condition. Let us suppose that we are interested in evaluating the irradiation hardening at low doses, namely below 1 dpa, in a regime where the irradiation hardening is of the order of few hundreds MPa. Let us further assume that the irradiation hardening is 100 MPa, corresponding, in our case, to a yield stress equals to 632 MPa, and that the irradiation induces a modest change in the post-yield behaviour, such that after irradiation the constitutive behaviour of the material correspond to Nr. 2. Estimating the yield stress by using the calibration between σ_y and P_y/t^2 for unirradiated materials would lead to a yield stress of 566 MPa, or in other words, to an irradiation hardening of 34 MPa, while 100 MPa are to be measured. This illustrates the need to establish another calibration for which the effects of the post-yield behaviour are minimized. This means, to establish a plot like that of Fig. 3, where the variable is not P_y/t^2 but another quantity to be derived from the ball punch test curve. The calibration we are after must have two characteristics: (i) the three data point sets corresponding to the three yield stress have to be as compact as possible with respect to the variable axis and (ii) they must be well separated with respect to each other.

The major difficulty in correlating P_y/t^2 to the yield stress arises from the fact that a significant volume of the disk, in particular below the ball, deforms plastically from the very beginning of the test. Therefore, P_y/t^2 should be relate to an averaged flow stress between 0 and 0.1 plastic strain, rather than to the yield stress. Thus, it would be more natural to search for a characteristic point of the punch curve at a lower deflection. Unfortunately, the punch test curve is extremely rounded from the very beginning, and no such point can be unambiguously identified. In a purely empirical way, we sought for a new parameter determined from the force–deflection curves that, at least for the strain hardening behaviour shown by the martensitic steel, replaces P_y and reduces the indetermination in yield stress characteristic of Fig. 3.

The procedure we used is illustrated in Fig. 4 where only the segments corresponding to the deflection range (0.05–0.2) of the punch test curves are shown. This deflection range was so selected since we observed that a linear fitting of the punch curve is quite satisfactory over it. From the extrapolation of the linear fits back to a zero deflection we can define a new parameter P_o (see Fig. 4) at the intersection with the y-axis. Clearly, the range of the scatter in P_o is smaller than that of P_y, suggesting that an influence of the initial post-yield behaviour remains even detectable in P_o; influence that we should try to remove from P_o. As a matter of

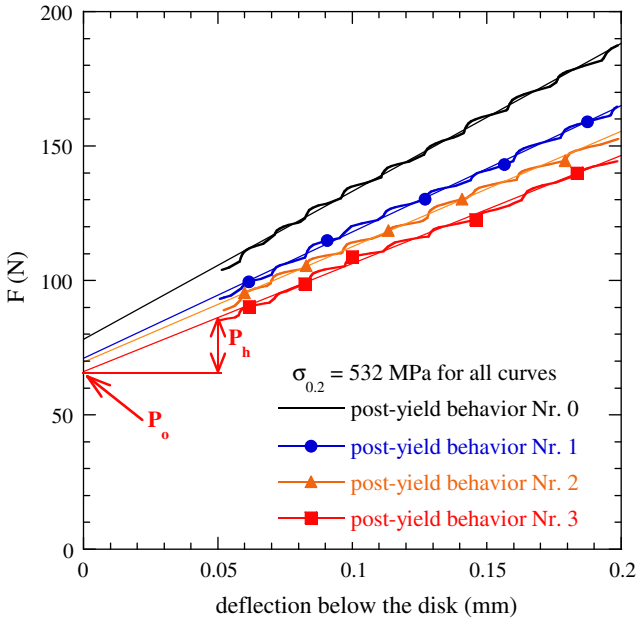

Fig. 4. Schematic view showing how P^* is defined: $P^* = P_o - P_h$.

fact, we observed that the larger P_o, the larger the slope of the fit of the punch test curves. This fact is related to an experimental observation on the proportionality between the SBPT curve slope and the average flow stress [7,13]. Therefore, it became natural to subtract from P_o a quantity proportional to the slope of the fit. After few attempts, we found that an appropriate quantity to subtract is P_h, defined by the product slope of the fit with a deflection equal to 0.05. So we defined P^* as (see Fig. 4):

$$P^* = P_o - P_h \tag{2}$$

where $P_h = 0.05 * S$, with S being the slope of the fit in the plastic bending regime. By doing so, a plot of σ_y versus P^*/t^2 yields a 'res-

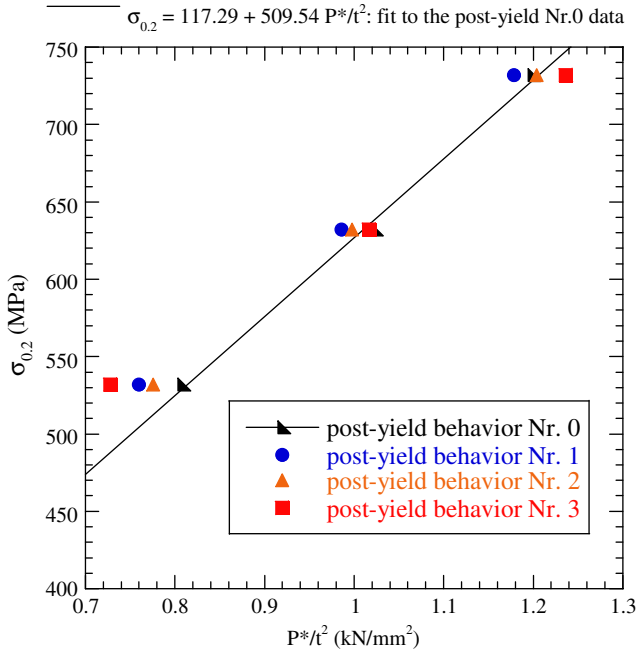

Fig. 5. $\sigma_{0.2}$ versus P^*/t^2 ($t = 0.250$ mm). The effects of the post-yield behaviour are minimized (compare with Fig. 3).

olution' on the assessed yield stress much better than the one given by P_y/t^2. A plot σ_y versus P^*/t^2 ($t = 0.25$ mm) is presented in Fig. 5. Again the fit on the plot has been done by taking into account only the data corresponding to the post-yield behaviour Nr. 0, considered as representative of the calibration that we would obtain on unirradiated materials. The scatter in P^*/t^2 has been significantly reduced with respect to that of P_y/t^2, which makes it reasonably independent of the post-yield behaviour while dependent enough on the yield stress level.

4. Conclusions

Finite element simulations of small ball punch tests were used to assess the flow properties of tempered martensitic steels. In the past, calibrations between the yield load P_y defined on the SBPT force–deflection curve was employed to correlate with the alloy yield stress. However this calibration suffers from the drawback of being, to some extent, dependent on the post-yield behaviour. Since the post-yield behaviour of the irradiated condition is in principle not known, this induces uncertainty in the assessment of the irradiation hardening. Based on careful analysis of the punch test deformation as seen by well validated finite element simulations, a new parameter was then proposed, that correlates with the yield stress and was shown to be much less dependent on post-yield behaviour, being thus more suited for post-irradiation examination studies.

Acknowledgments

The financial support of the Swiss National Foundation and of EURATOM is gratefully acknowledged. This work, supported by the European Communities under the contract of Association between EURATOM/(Switzerland), was carried out within the framework of the European Fusion Development Agreement (EFDA). The views and opinions expressed herein do not necessarily reflect those of the European Commission. The Paul Scherrer Institute is acknowledged for providing access to its facility.

References

[1] P. Spätig, G.R. Odette, G.E. Lucas, M. Victoria, J. Nucl. Mater. 307–311 (2002) 536.
[2] R. Bonadé, P. Spätig, R. Schaublin, M. Victoria, Mater. Sci. Eng. A 387–389 (2004) 16.
[3] R. Klueh, D.S. Gelles, S. Jitsukawa, A. Kimura, G.R. Odette, B. Van der Schaaf, M. Victoria, J. Nucl. Mater. 307–311 (2002) 455.
[4] P. Spätig, N. Baluc, M. Victoria, Mater. Sci. Eng. A 309–310 (2001) 425.
[5] E.N. Campitelli, P. Spätig, R. Bonadé, W. Hoffelner, M. Victoria, J. Nucl. Mater. 335 (2004) 3666.
[6] E.N. Campitelli, P. Spätig, J. Bertsch, C. Hellwig, Mater. Sci. Eng. A 400&401 (2005) 386.
[7] P. Spätig, E.N. Campitelli, R. Bonadé, N. Baluc, Nucl. Fusion 45 (2005) 635.
[8] Y. Ruan, P. Spätig, M. Victoria, J. Nucl. Mater. 307–311 (2002) 236.
[9] X. Mao, H. Takahashi, J. Nucl. Mater. 150 (1987) 42.
[10] T.S. Byun, K. Farrell, Acta Mater. 52 (2004) 1597.
[11] Z. Yao, R. Schäublin, P. Spätig, M. Victoria, Philos. Mag. 85 (2005) 745.
[12] G.R. Odette, M.Y. He, E.G. Donahue, P. Spätig, T. Yamamoto, J. Nucl. Mater. 307–311 (2002) 171.
[13] E.N. Campitelli; PhD thesis n° 3304; EPFL, Laussane, 2005.